CrossMark

ORIGINAL PAPER

Aptasensor for visual and fluorometric determination of lysozyme based on the inner filter effect of gold nanoparticles on CdTe quantum dots

Luping Chen[1] · Ning Xia[2] · Tingting Li[1] · Yanhua Bai[1] · Xiaolan Chen[1]

Abstract The authors describe an aptasensor for visual and fluorescent detection of lysozyme via an inner filter effect (IFE). The assay is based on the fact that red gold nanoparticles (AuNPs) act as powerful absorbers of the green fluorescence of CdTe because of spectral overlap. If the lysozyme-binding aptamer is adsorbed onto the surface of the AuNPs, the salt-induced aggregation of AuNPs (that leads to a color change from red to blue) does not occur and the IFE remains efficient. If lysozyme is present, it will bind the aptamer and thereby prevent its adsorption on the AuNPs. As a result, the salt-triggered aggregation of the AuNPs will occur. Consequently, color will change from red to blue, and green fluorescence will pop up because the IFE is suppressed. Under optimum conditions, fluorescence is linearly related to lysozyme concentration in the 1.0 nM to 20 nM concentration range, with a 0.55 nM limit of detection. The method is perceived to be of wider applicability in that it may be used to design other visual and fluorescent assays if appropriate aptamers are available.

✉ Xiaolan Chen
chenxiaolan@xtu.edu.cn

Luping Chen
hxlupingchen@163.com

1 Key Laboratory of Environmentally Friendly Chemistry and Applications of Ministry of Education, College of Chemistry, Xiangtan University, Xiangtan, Hunan 411105, China

2 College of Chemistry and Chemical Engineering, Anyang Normal University, Anyang, Henan 455000, China

Introduction

Lysozyme is an antimicrobial protein that contains 129 amino acid residues with a molecular weight of approximately 14.4 kD [1]. As an important defense molecule of the innate immune system, lysozyme widely distributed in tissues and secretions of mammals [2]. Increased concentration of lysozyme in serum and urine is related to many diseases, such as leukemia, renal diseases, and meningitis [3, 4]. Therefore, the level of lysozyme has been used as an importance clinical index in the diagnosis, treatment and monitoring the progression of related diseases. Practical methods with high selectivity and sensitivity for simple and rapid detection of lysozyme are of considerable importance. A variety of techniques have been used for lysozyme protein assay, including but not limited to fluorescence detection [5–8], electrochemical detection [9], electrochemiluminescence aptasensor [10], molecular imprinting [11], surface enhanced Raman scattering [12], series piezoelectric quartz crystal sensor (SPQC) [13] and colorimetric assay [14]. Most of these methods have high sensitivity and selectivity, but require costly bio-molecular reagents, expensive instrumentation, and/or time-consume immobilizing processes.

Aptamers are single-stranded oligonucleotides that have been designed through an in-vitro selection process called SELEX (Systematic Evolution of Ligands by Exponential Enrichment) [15, 16]. They can bind a variety of target molecules with high affinity and specificity, such as peptides, amino acids, proteins, and even organic/inorganic molecules [17]. Compared with antibodies, aptamers hold many advantageous characteristics, including simple and reproducible

⚓ Springer

synthesis, easy and controllable labeling, long-term stability and design flexibility [18]. Aptamers constitute a promising alternative to antibodies in target molecule recognition and sensing [19].

Quantum dots (QDs) are semiconductor nanocrystals with unique optical properties, such as high quantum yields, long fluorescence lifetimes, size-dependent emission, pronounced photostability, and broad absorption spectra coupled with narrow fluorescence emission spectra [20]. Gold nanoparticles (AuNPs), another versatile nanomaterial, have been broadly used in the development of colorimetric and fluorescence-based analytical methods, owing to their high extinction coefficients and strong distance dependent optical properties [21]. Many studies reported that AuNPs can quench the fluorescence of QDs through fluorescence resonance energy transfer (FRET) [22]. Typically, the design of FRET process would require a particular distance or geometry between AuNPs and QDs to ensure the valid interaction [23]. Therefore, it is necessary and important for AuNPs or QDs to be modified or engineered to establish the FRET-based methods, which is complicated and time-consuming and therefore to restricted practical applications.

The inner filter effect (IFE) of fluorescence refers to the absorption of the excitation and/or emission of fluorophores by absorbers in the detection system [24]. Compared to the conventional FRET, the IFE method does not require the intermolecular connection of fluorophores and absorbers at a particular distance, providing a comparatively simple and facile approach for the analytical detection [25]. As an efficient strategy of fluorescent method, the IFE has been applied for various analytes detections [26–29].

Herein, we developed a label-free aptamer sensing strategy for visual and fluorescent detection of lysozyme based on AuNPs colorimetry and the IFE of AuNPs on the fluorescence of CdTe QDs. The method offers considerable flexibility and high simplicity because it obviates the need of modified aptamers and does not require the modification of AuNPs to link CdTe QDs. Moreover, to the best of our knowledge, little has been reported on the visual and fluorescent detection of lysozyme based on the IFE of AuNPs on QDs.

Materials and methods

Chemicals

Trisodium citrate ($Na_3C_6H_5O_7 \cdot 2H_2O$, 99.0 %), cadmium chloride ($CdCl_2$, 99.99 %), tellurium powder (Te, 99.997 %), sodium borohydride ($NaBH_4$, 98 %), and glutathione (GSH, 95 %) were purchased from Sigma-Aldrich (http://www.sigmaaldrich.com), chloroauric acid ($HAuCl_4$)

was purchased from Beijing Dingguo Changsheng Biotechnology Company (Beijing, China, http://www.dingguo.com). Bovine serum albumin (BSA), immunoglobin G (IgG), thrombin, adenosine, cysteine, lysozyme and lysozyme-binding aptamer (5′-ATC AGG GCT AAA GAG TGC AGA GTT ACT TAG-3′) were purchased from Sangon Biotechnology Co. (Shanghai, China, http://www.sangon.com). All reagents and solvents were at least analytical grade and used directly without further purification. Other reagents were obtained from Sinopharm Chemical Reagent Co., Ltd. (Shanghai, China, http://www.sinoreagent.com). All solutions were prepared with ultrapure water (18.2 MΩ cm) from a Millipore system.

Apparatus

The fluorescence spectra were obtained by using a RF-5301 PC spectrofluorophotometer (Shimadzu, Japan) with a $3 \times 10 \times 45$ mm quartz cuvette. UV-vis spectra were obtained on a Shimadzu UV-2450 PC spectrophotometer (Shimadzu, Japan). Dynamic light scattering (DLS) and zeta potentials (ζ) were measured on a Malvern Zetasizer Nano ZEN3690. (Malvern, UK). All pH measurements were made with a PHS-3C pH meter (Tuopu Co., Hangzhou, China).

Synthesis of CdTe QDs

Water-soluble GSH-capped CdTe QDs were prepared according to the procedure reported by Li et al. with some modifications [24]. The whole synthetic process was carried out under the protection of N_2. Fresh sodium hydrogen telluride (NaHTe) solution was made before synthesis by dissolving 0.025 g of sodium borohydride ($NaBH_4$) in 1.0 mL of deionized water followed by the addition of 0.040 g of tellurium powder, and the solution was heated at 60 °C for 40 min. The $CdCl_2$-GSH stock solution was prepared by dissolving 14.3 mg of $CdCl_2$ and 16 mg of GSH in 50 mL of deionized water, and the pH was adjusted to 9.0 with sodium hydroxide before use. Then, 100 μL of the freshly prepared NaHTe solution was mixed with the $CdCl_2$-GSH stock solution. The reaction mixture was then subjected to a reflux of 100 °C and reacted for 30 min before cooling to room temperature. For the purification of CdTe QDs, a dialysis membrane with a molecular weight of cutoff 8000 was used in 0.01 M NaOH solution for 2 days to remove the free $CdCl_2$ and GSH [28]. The as prepared GSH-capped CdTe QDs were characterized by UV-vis spectroscopy, fluorescence emission spectrum, and zeta potential measurement analyzer. According to the calculation method mentioned in a previous research [30], the concentration of CdTe QDs was calculated to be 7.00 μM.

Synthesis of AuNPs

Citrate-stabilized AuNPs were prepared by following Frens' method, as reported previously [31] with minor modifications. All glassware used in the experiment was soaked in aqua regia, rinsed thoroughly with water, and oven-dried prior to use. Briefly, 100 mL $HAuCl_4$ (0.01 %, w/w) was heated to boiling with stirring, and then 2.0 mL trisodium citrate solution (1 %, w/w) was added quickly. After the color change from pale yellow to deep red, the solution was refluxed for an additional 5 min and left to cool to room temperature. Then, the solution was stored at 4 °C for further utilization. The final concentration of AuNPs was calculated to be 1.49 nM from the UV − vis absorption spectrum based on an extinction coefficient of 3.24×10^8 mol^{-1} cm^{-1} at λ_{520} for AuNPs [32].

Detection method

First, 60 μL 1.0 μM lysozyme-binding aptamer solution was mixed with different concentrations of lysozyme solution. The mixture was incubated with 600 μL of AuNPs at room temperature for 30 min. Then, the above solution was mixed with 100 μL phosphate buffer (10 mM, pH 8.5) which contains 0.6 M NaCl. Double distilled water was added to each of the test tubes to make up to a final volume of 1.0 mL. After 30 min reaction, the color change of the mixture solution was recorded by a digital camera and the absorbance spectra of the mixture solution were recorded with a UV-vis spectrophotometer. Then 6 μL of CdTe QDs was added to the above solution. After reaction for 100 s, the emission spectroscopy measurements

were recorded with the excitation wavelength at 324 nm. The fluorescence data were analyzed by plotting the relative fluorescence intensity F/F_0 (F_0 and F are the fluorescence intensity of the CdTe QDs in the absence and presence of lysozyme, respectively) at 512 nm versus the concentration of lysozyme.

Results and discussion

The principle of the protocol

The principle of our experimental design is illustrated in Scheme 1. Lysozyme-binding aptamers adsorbed to the surface of AuNPs, preventing NaCl-induced aggregation of AuNPs. The fluorescence emission of CdTe QDs was then quenched significantly by the dispersed AuNPs due to the IFE. Upon the addition of lysozyme, lysozyme-binding aptamers interacted specifically with lysozyme, losing the capability to stabilize AuNPs. This caused the aggregation of AuNPs and the color change from red to blue. Furthermore, the IFE of AuNPs on CdTe QDs was weakened and the fluorescence intensity of CdTe QDs was recovered.

Characterization of CdTe QDs and AuNPs

From Fig. 1, we found that the UV–vis absorption spectrum of dispersed AuNPs displayed intense characteristic absorption peak at 520 nm, while the absorption of aggregated AuNPs at 520 nm was very weak. The fluorescence spectrum of CdTe QDs showed a well emission bands under a single wavelength

Scheme 1 Illustration of the visual and fluorescent detection of lysozyme through the inner filter effect (IFE)of AuNPs on QDs
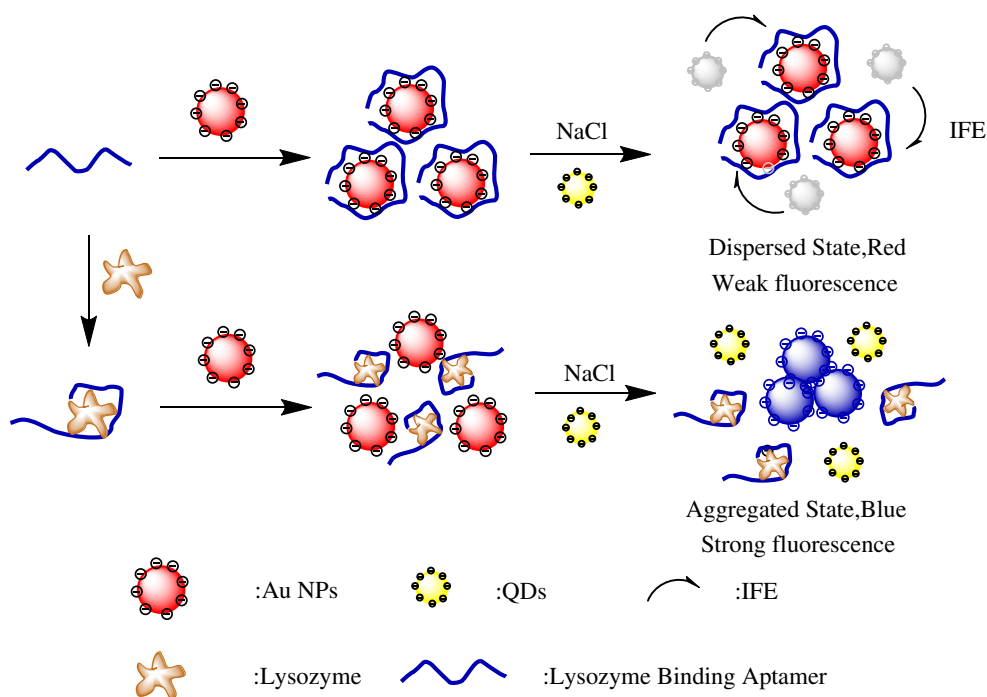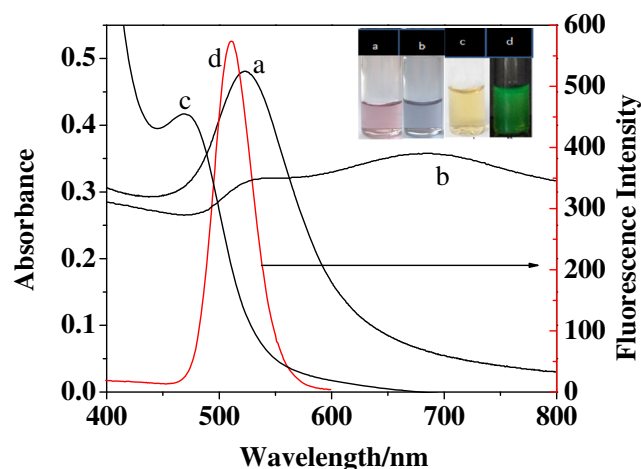
Fig. 1 UV–vis absorption spectra of AuNPs in dispersed (**a**) and aggregated (**b**) state as well as CdTe QDs (7.00 μM) (**c**). Curve d shows the fluorescence emission spectra of CdTe QDs (0.042 μM). The inset shows the photos of AuNPs in dispersed (**a**) and aggregated (**b**) state, as well as CdTe QDs under sunlight (**c**) and under UV lamp (**d**). The concentration of AuNPs is 0.89 nM

excitation at 324 nm, and the fluorescence emission maximum were around 512 nm. The inset in Fig. 1 shows the photos of the dispersed and aggregated AuNPs, as well as CdTe QDs under sunlight and UV lamp. Dynamic light scattering (DLS)
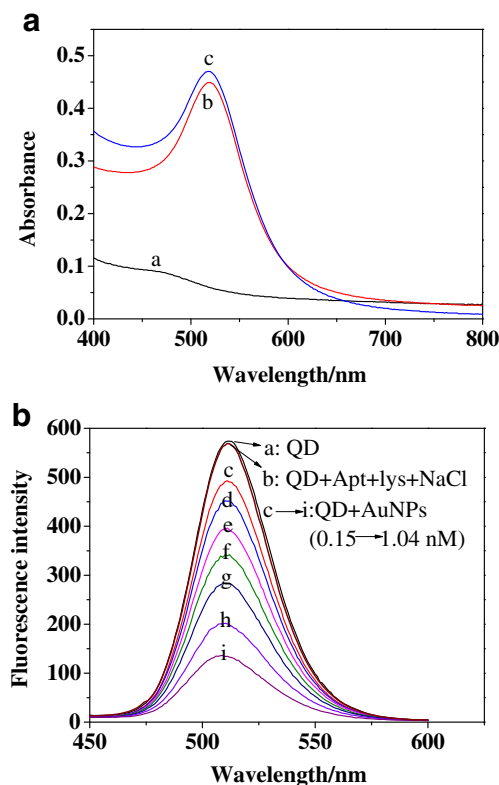

Fig. 2 (**A**) The absorption spectra of CdTe QDs (**a**), AuNPs (**b**) and the mixture of CdTe QDs and AuNPs. The concentration of CdTe QDs and AuNPs is 0.042 μM and 0.89 nM, respectively. The pH is 8.5. (**B**) The fluorescence spectra of 0.042 μM CdTe QDs in the presence of different concentration of AuNPs (0, 0.15, 0.30, 0.45, 0.60, 0.75, 0.89 and 1.04 nM)

images of the prepared AuNPs and CdTe QDs are shown in Fig. S1A. The DLS images revealed that the average diameter of the AuNPs and CdTe QDs were 16.9 ± 1.2 nm and 3.29 ± 0.45 nm, respectively. Besides, the zeta potential (ζ) of the dispersed AuNPs was measured to be -41.7 ± 6.0 mV due to the negatively charged capping reagent of citrate ion. The ζ of CdTe QDs was -43.4 ± 4.2 mV (Fig. S1B) at pH 8.5 due to the ionization of the –COOH group in GSH (pI =5.93). Both AuNPs and CdTe QDs showed negative zeta potentials at pH 8.5.

Effects of AuNPs on the fluorescence intensity of CdTe QDs

As reported previously, IFE would occur effectively only if the absorption band of the absorber possesses a complementary overlap with the excitation and/or emission bands of the
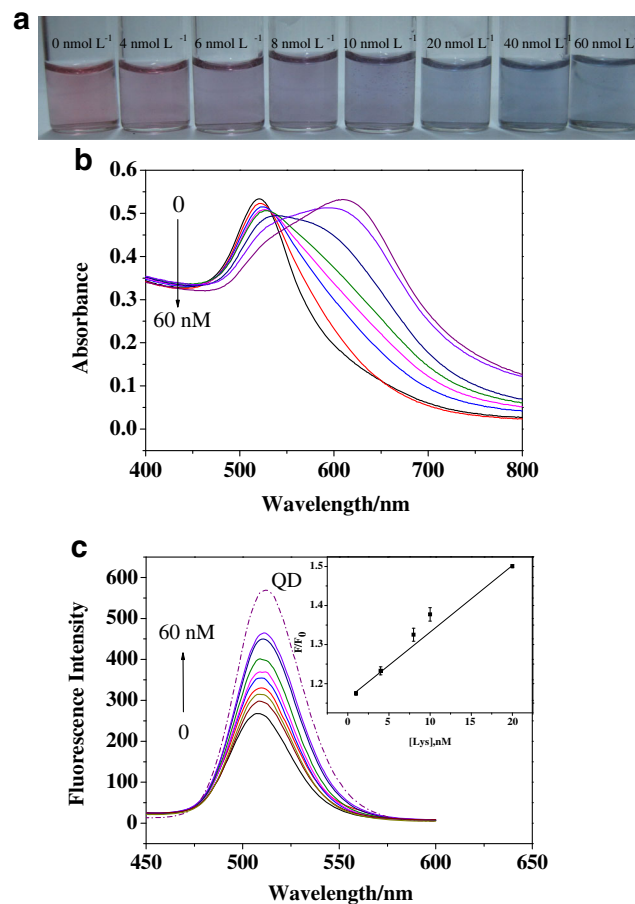

Fig. 3 The photographic images (**a**) and UV-vis absorption spectra (**b**) of aptamer-AuNPs under different concentrations of lysozyme (0, 4.0, 6.0, 8.0, 10, 20, 40 and 60 nM) ($n = 3$). The concentrations of aptamers and AuNPs are 60 nM and 0.89 nM, respectively. (**c**) The fluorescence spectra of aptamer-AuNPs-CdTe QDs system in the presence of different concentrations of lysozyme (0, 0.1, 1.0, 4.0, 8.0, 10, 20, 40 and 60 nM) ($n = 3$). Inset: the linear plots of F/F_0 versus the concentrations of lysozyme (1.0, 4.0, 8.0, 10 and 20 nM). The concentrations of aptamers, AuNPs, NaCl and CdTe QDs are 60 nM, 0.89 nM, 0.06 M and 0.042 μM, respectively

Table 1 Comparison of performance of different lysozyme assays

Method	Linear range (nmol L^{-1})	LOD (nmol L^{-1})	References
Fluorescence detection (CuInS$_2$ QDs)	40–1000		[5]
Fluorescence method (MC–Eu^{3+})	0–35,000	474	[6]
Fluorescence detection (CMCS- QDs)	0.007–0.08	0.0022	[7]
Fluorescence anisotropic sensing detection	12.5–300	4.9	[8]
Electrochemical method	20–840	30	[9]
Electrogenerated chemiluminescence	0.64–640	0.12	[10]
Molecular imprinting	6940–69,400		[11]
Surface enhanced Raman scattering		3470	[12]
SPQC	1–80	0.5	[13]
Colorimetric assay	35–1050	35 (bare eye)	[14]
Fluorescence detection (IFE)	1–20	0.55	This work
Colorimetric assay	4.0–60	4.0 (bare eye)	This work

fluorophore [27, 29], though there are no chemical linkage between absorber and fluorophore. As shown in Fig. 1, the absorption spectrum of the dispersed but not aggregated AuNPs overlaps very well with the fluorescence emission spectrum of CdTe QDs at 520 nm. In addition, the absorption spectra of AuNPs remained unchanged in the presence of CdTe QDs (Fig. 2A), suggesting that no electrostatic attractive interaction or rare energy transfer between the CdTe QDs and AuNPs [33]. This can be explained by the fact that both AuNPs and CdTe QDs showed negative zeta potentials at pH 8.5 [24]. To further demonstrate the generality of our design using AuNPs as an IFE-absorber and CdTe QDs as an IFE-fluorophore, the fluorescence spectra of CdTe QDs mixed with different concentrations of AuNPs were collected. From Fig. 2B, it can be observed that the fluorescence intensity of CdTe QDs continuously decreased with the increase of AuNPs concentration from 0 to 1.04 nM.

Optimization for lysozyme detection

For lysozyme detection, the following parameters were optimized: (a) concentrations of CdTe QDs and AuNPs; (b)

concentration of NaCl; (c) concentration of lysozyme-binding aptamer; (d) Sample pH value and the reaction time. Respective data and Figures are given in the Electronic Supporting Material. The following experimental conditions were found to give best results: (a) 0.042 μM CdTe QDs and 0.89 nM AuNPs; (b) 0.06 M of NaCl; (c) 60 nM aptamer; (d) sample pH value of 8.5 and the reaction time of 100 s.

Lysozyme detection

It can be seen from Fig. 3a that the color of the AuNPs solution changes from red to blue gradually upon increasing the concentration of lysozyme from 4.0 to 60 nM. According to the previous reports [34], single-stranded oligonucleotides (ssDNA) are adsorbed on the surface of AuNPs due to van der Waals force. This prevents the NaCl-induced aggregation of AuNPs. In the absence of lysozyme, lysozyme-binding aptamers (ssDNA) enhance the stability of AuNPs and prevent their NaCl-induced aggregation. The color of the solution remains red. In the presence of lysozyme, lysozyme-binding aptamers lose their ability to protect AuNPs against the NaCl-induced aggregation AuNPs. As a result, a significant color change of the solution from red to blue is observed. The UV-
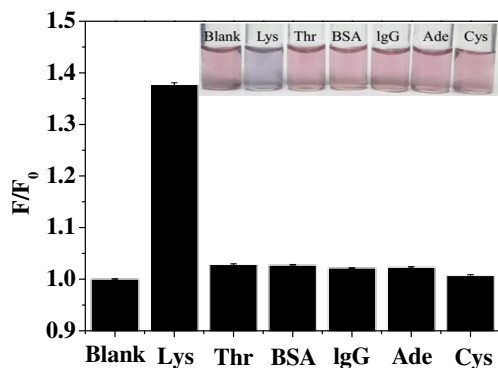

Fig. 4 Selectivity of the visual and fluorescent assay to lysozyme (n = 3). The concentration of lysozyme and the interfering substances was kept at 10 nM

Table 2 Detection of lysozyme in the spiked samples (n = 3)

Sample	Found (nmol L^{-1})	Added (nmol L^{-1})	Measured (nmol L^{-1})	Recovery (%)	RSD (%)
1[a]	2.57	1.00	3.59	102.0	2.7
		2.00	4.58	100.5	4.6
		5.00	7.30	94.6	0.9
2[b]	1.23	1.00	2.16	93.0	3.4
		2.00	3.26	101.5	4.4
		5.00	6. 11	97.6	5.7

[a] tear sample

[b] saliva sample

vis spectra investigations reveal that with the increase of lysozyme concentration, the red-shifted band corresponding to the aggregated AuNPs was intensified, which was accompanied by a decrease of absorbance at 520 nm (Fig. 3b). Figure 3a shows that the color change can be easily seen with bare eyes if the analyte concentration is exceeding 4.0 nM. Compared with target-induced charge reduction of aptamers for visual detection of lysozyme [14], the method exhibiting higher sensitivity in visual detection of lysozyme.

Moreover, an enhanced sensitivity fluorescence detection of lysozyme was achieved via the IFE of AuNPs on the fluorescence of CdTe QDs. Since the changes in the absorbance of the absorber translate into exponential changes in fluorescence of the fluorophore, the fluorescence signal is more sensitive over that of the absorptiometry [35]. In the absence of lysozyme, the AuNPs were dispersed in NaCl solution, resulting in significant fluorescence quenching of CdTe QDs via the IFE. Upon the addition of lysozyme, the lysozyme-binding aptamers associated with the targets, leading to the aggregation of AuNPs in NaCl solution and the efficiency of the IFE is reduced. The fluorescence intensity of CdTe QDs is continuously recovered with the increasing concentration of lysozyme. A good linear relationship between the fluorescence intensity ratio F/F_0 and the concentration of lysozyme was obtained in the range from 1.0 to 20 nM (Fig. 3c). The regression equation is $F/F_0 = 1.1618 + 0.0170$ [lysozyme] (nM), where F_0 and F are the fluorescence intensity of the CdTe QDs in the absence and presence of lysozyme, respectively. The corresponding regression coefficient is 0.998, and the LOD (3σ) for lysozyme is 0.55 nM. Compared with the existing methods (Table 1), the method shows a comparable quantification range and LOD for visual and fluorescent detection of lysozyme.

To explore the feasibility of the methods, five potentially interfering materials (BSA, IgG, thrombin, adenosine and cysteine) were chosen for the interference study. As shown in Fig. 4, all of these potentially interfering proteins did not cause a significant increase in F/F_0. The color of lysozyme sample changed to blue, but that of other samples remained red. The results confirmed that the established aptamer-AuNPs-CdTe QDs IFE method showed extraordinary selectivity towards lysozyme. The selectivity is attributed to the fact that lysozyme-binding aptamers bind to lysozyme with high affinity.

Analysis lysozyme in real samples

To verify the practicality of this method, the concentrations of lysozyme in tear and saliva samples were determined. The tear and saliva samples were collected from healthy volunteers between 8.30 and 10.30 a.m. The tear samples were directly diluted 500 times with double distilled water, while the saliva samples were centrifuged at 10, 000 rpm for 30 min to remove cellular debris and diluted 30 times with double distilled water [13]. Specifically, different concentrations of lysozyme were added to 10 μL resulting sample solution, respectively. The above sample solutions were then used for fluorescence analysis. As shown in Table 2, the average recoveries in these spiked samples are in the range of 90.4 ~ 102.0 % and the RSDs are all lower than 5.7 %. This is indicative of the potential applicability of the aptamer-AuNPs-CdTe QDs system for lysozyme detection in real samples.

Conclusion

In summary, we reported a label-free aptasensor for visual and fluorescent detection of lysozyme based on the IFE of AuNPs on the fluorescence of CdTe QDs. The method shows several analytical advantages: (1) the method has high sensitivity and enables accurate quantification of lysozyme as low as 4.0 nM (visual) and 0.55 nM (fluorescent), respectively; (2) the direct visualization of lysozyme by the bare eye obviates the need of any special equipment; (3) the strategy exhibits excellent selectivity for lysozyme over other materials due to the specific recognition of lysozyme-binding aptamers with lysozyme; (4) the method does not need to modify AuNPs or label aptamers. Furthermore, the method was successfully applied to analyze lysozyme in the tear and saliva samples. We believe that the strategy would be helpful for the sensitive and selective detection of other biomolecules by choosing the specific aptamers for the target biomolecules.

Compliance with ethical standards We declare that we have no competing interests.

References

1. Jollès, P (1969) Lysozymes: a chapter of molecular biology. Angewandte Chemie International Edition in English 8:227–239
2. Tohidi Moghadam T, Ranjbar B (2015) Heat induced aggregation of gold nanorods for rapid visual detection of lysozyme. Talanta 144:778–787
3. Levinson SS, Elin RJ, Yam L (2002) Light chain proteinuria and lysozymuria in a patient with acute monocytic leukemia. Clin Chem 48:1131–1132
4. Manifold I, Bishop F, Cloke P, Triger D, Underwood J (1982) Lysozyme in chronic liver disease: a biochemical and histological study. J Clin Pathol 35:815–819
5. Liu S, Na W, Pang S, Shi F, Su X (2014) A label-free fluorescence detection strategy for lysozyme assay using $CuInS_2$ quantum dots. Analyst 139:3048–3054
6. Chongqiu J, Li L (2004) Lysozyme enhanced europium–metacycline complex fluorescence: a new spectrofluorimetric method for the determination of lysozyme. Anal Chim Acta 511:11–16

7. Yu S, Yang L, Ziping L, Linlin L, Xinyan W, Xingguang S, Qiang M (2014) A novel ultrasensitive carboxymethyl chitosan-quantum dot-based fluorescence " on-off" nanosensor for lysozyme detection. Biosens Bioelectron 61:9–13

8. Mingjian Z, Yang C, Xiao X, Hongduan H, Feng L, Na L (2012) The homogeneous fluorescence anisotropic sensing of salivary lysozyme using the 6-carboxyfluorescein-labeled DNA aptamer. Biosens Bioelectron 32:148–154

9. Felisilda BMB, Alvarez de Eulate E, Arrigan DWM (2015) Investigation of a solvent-cast organogel to form a liquid-gel microinterface array for electrochemical detection of lysozyme. Anal Chim Acta 893:34–40

10. Yan L, Honglan Q, Qiang G, Chengxiao Z (2011) Label-free and sensitive electrogenerated chemiluminescence aptasensor for the determination of lysozyme. Biosens Bioelectron 26:2733–2736

11. Huachang C, Juan K, Dongying Y, Guoqi F (2014) Synthesis of surface molecularly imprinted nanoparticles for recognition of lysozyme using a metal coordination monomer. Biosens Bioelectron 53:5–11

12. Kahraman M, Wachsmann-Hogiu S (2015) Label-free and direct protein detection on 3D plasmonic nanovoid structures using surface-enhanced Raman scattering. Anal Chim Acta 856:74–81

13. Yan L, Fengjiao H, Xianwen M, Feifei T, Xiaohong S (2014) Lysozyme aptamer biosensor based on electron transfer from SWCNTs to SPQC-IDE. Sensors Actuators B 199:377–383

14. Su J, Zhou W, Xiang Y, Yuan R, Chai Y (2013) Target-induced charge reduction of aptamers for visual detection of lysozyme based on positively charged gold nanoparticles. Chem Commun 49: 7659–7661

15. Tuerk C, Gold L (1990) Systematic evolution of ligands by exponential enrichment: RNA ligands to bacteriophage T4 DNA polymerase. Science 249:505–510

16. Wu J, Zhu Y, Xue F, Mei Z, Yao L, Wang X, Zheng L, Liu J, Liu G, Peng C (2014) Recent trends in SELEX technique and its application to food safety monitoring. Microchim Acta 181:479–491

17. Yin W, Ji Z, Xu W, Yixiang D (2015) Amplified fluorescent aptasensor through catalytic recycling for highly sensitive detection of ochratoxin A. Biosens Bioelectron 65:16–22

18. Yunying X, Wenjiao Z, Ming Z, Yun X, Ruo Y, Yaqin C (2015) Toehold strand displacement-driven assembly of G-quadruplex DNA for enzyme-free and non-label sensitive fluorescent detection of thrombin. Biosens Bioelectron 64:306–310

19. Lee SE, Chen Q, Bhat R, Petkiewicz S, Smith JM, Ferry VE, Correia AL, Alivisatos AP, Bissell MJ (2015) Reversible aptamer-au plasmon rulers for secreted single molecules. Nano Lett 15: 4564–4570

20. Wang K, Qian J, Jiang D, Yang Z, Du X, Wang K (2015) Onsite naked eye determination of cysteine and homocysteine using quencher displacement-induced fluorescence recovery of the dual-emission hybrid probes with desired intensity ratio. Biosens Bioelectron 65:83–90

21. Yun W, Jiang J, Cai D, Zhao P, Liao J, Sang G (2016) Ultrasensitive visual detection of DNA with tunable dynamic range by using un-modified gold nanoparticles and target catalyzed hairpin assembly amplification. Biosens Bioelectron 77:421–427

22. Shi Y, Pan Y, Zhang H, Zhang Z, Li M-J, Yi C, Yang M (2014) A dual-mode nanosensor based on carbon quantum dots and gold nanoparticles for discriminative detection of glutathione in human plasma. Biosens Bioelectron 56:39–45

23. Chen G, Song F, Xiong X, Peng X (2013) Fluorescent nanosensors based on fluorescence resonance energy transfer (FRET). Ind Engi Chem Res 52:11228–11245

24. Li J, Li X, Shi X, He X, Wei W, Ma N, Chen H (2013) Highly sensitive detection of caspase-3 activities via a nonconjugated gold nanoparticle–quantum dot pair mediated by an inner-filter effect. ACS Appl Mater Interfaces 5:9798–9802

25. Yan X, Li H, Han X, Su X (2015) A ratiometric fluorescent quantum dots based biosensor for organophosphorus pesticides detection by inner-filter effect. Biosens Bioelectron 74:277–283

26. Saleh SM, Ali R, Hirsch T, Wolfbeis OS (2011) Detection of biotin–avidin affinity binding by exploiting a self-referenced system composed of upconverting luminescent nanoparticles and gold nanoparticles. J Nanopart Res 13:4603–4611

27. Cao X, Shen F, Zhang M, Sun C (2014) Rapid and highly-sensitive melamine sensing based on the efficient inner filter effect of Ag nanoparticles on the fluorescence of eco-friendly ZnSe quantum dots. Sensors Actuators B Chem 202:1175–1182

28. Xu L, Li B, Jin Y (2011) Inner filter effect of gold nanoparticles on the fluorescence of quantum dots and its application to biological aminothiols detection. Talanta 84:558–564

29. Yan X, Li H, Li Y, Su X (2014) Visual and fluorescent detection of acetamiprid based on the inner filter effect of gold nanoparticles on ratiometric fluorescence quantum dots. Anal Chim Acta 852: 189–195

30. Yu WW, Qu L, Guo W, Peng X (2003) Experimental determination of the extinction coefficient of cdte, cdse, and CdS nanocrystals. Chem Mater 15:2854–2860

31. Grabar KC, Brown KR, Keating CD, Stranick SJ, Tang S-L, Natan MJ (1997) Nanoscale characterization of gold colloid monolayers: a comparison of four techniques. Anal Chem 69:471–477

32. Haiss W, Thanh NTK, Aveyard J, Fernig DG (2007) Determination of size and concentration of gold nanoparticles from uv−vis spectra. Anal Chem 79:4215–4221

33. Chang H-C, Ho J-A (2015) Gold nanocluster-assisted fluorescent detection for hydrogen peroxide and cholesterol based on the inner filter effect of gold nanoparticles. Anal Chem 87:10362–10367

34. Gopinath SCB, Lakshmipriya T, Awazu K (2014) Colorimetric detection of controlled assembly and disassembly of aptamers on unmodified gold nanoparticles. Biosens Bioelectron 51:115–123

35. Shao N, Zhang Y, Cheung S, Yang R, Chan W, Mo T, Li K, Liu F (2005) Copper ion-selective fluorescent sensor based on the inner filter effect using a spiropyran derivative. Anal Chem 77: 7294–7303